⌘ *Author's Choice*

THE JOURNAL OF BIOLOGICAL CHEMISTRY VOL. 286, NO. 47, pp. 40934–40942, November 25, 2011
Printed in the U.S.A.

Flexible Cullins in Cullin-RING E3 Ligases Allosterically Regulate Ubiquitination*[S]

Received for publication, June 29, 2011, and in revised form, September 8, 2011 Published, JBC Papers in Press, September 20, 2011, DOI 10.1074/jbc.M111.277236

Jin Liu[‡] **and Ruth Nussinov**[‡§1]

From the [‡]*Basic Science Program, SAIC-Frederick, Incorporated, Center for Cancer Research Nanobiology Program, NCI-Frederick, National Institutes of Health, Frederick, Maryland 21702 and the* [§]*Sackler Institute of Molecular Medicine, Department of Human Genetics and Molecular Medicine, Sackler School of Medicine, Tel Aviv University, Tel Aviv 69978, Israel*

Background: Protein ubiquitination regulates critical biological processes, including degradation of malfunctioning proteins.
Results: We show that Cul1, Cul4A, and Cul5 are not rigid. All are flexible scaffolds with preferred distributions of conformational states.
Conclusion: Cullin flexibilities are regulated allosterically, allowing the cullin-RING E3 ubiquitin ligases to increase the E2-substrate distance to a specific range, facilitating polyubiquitination.
Significance: Cullins are not inert scaffolds and allosterically regulate ubiquitination.

How do the cullins, with conserved structures, accommodate substrate-binding proteins with distinct shapes and sizes? Cullin-RING E3 ubiquitin ligases facilitate ubiquitin transfer from E2 to the substrate, tagging the substrate for degradation. They contain substrate-binding, adaptor, cullin, and Rbx proteins. Previously, we showed that substrate-binding and Rbx proteins are flexible. This allows shortening of the E2-substrate distance for initiation of ubiquitination or increasing the distance to accommodate the polyubiquitin chain. However, the role of the cullin remained unclear. Is cullin a rigid scaffold, or is it flexible and actively assists in the ubiquitin transfer reaction? Why are there different cullins, and how do these cullins specifically facilitate ubiquitination for different substrates? To answer these questions, we performed structural analysis and molecular dynamics simulations based on Cul1, Cul4A, and Cul5 crystal structures. Our results show that these three cullins are not rigid scaffolds but are flexible with conserved hinges in the N-terminal domain. However, the degrees of flexibilities are distinct among the different cullins. Of interest, Cul1 flexibility can also be changed by deletion of the long loop (which is absent in Cul4A) in the N-terminal domain, suggesting that the loop may have an allosteric functional role. In all three cases, these conformational changes increase the E2-substrate distance to a specific range to facilitate polyubiquitination, suggesting that rather than being inert scaffold proteins, cullins allosterically regulate ubiquitination.

Protein ubiquitination regulates critical biological processes, including degradation of malfunctioning or damaged proteins in cells and regulation of cell signaling pathways (1, 2). The target substrate proteins are ubiquitinated via a three-enzyme cascade. In the first step, ubiquitin forms a covalent bond with the ubiquitin-activating enzyme (E1). The second step is to transfer ubiquitin from E1 to ubiquitin-conjugating enzyme (E2). The E3 ubiquitin ligases catalyze the final step, bringing E2 and the substrate into proximity to facilitate ubiquitin transfer from E2 to the substrate. The substrate, labeled with a ubiquitin chain, is then recognized and degraded by the proteasome (3).

The E3 ubiquitin ligases are the most diverse enzymes in the ubiquitination pathway due to their specificity in recognizing thousands of substrates. Based on how ubiquitin is transferred, the E3 ubiquitin ligases can be divided into two major classes: HECT E3 and RING E3. The cullin-RING E3 ubiquitin ligases (CRLs),[2] which include ~400 family members, represent one of the largest superfamilies in RING E3 ligases (4). It has been estimated that CRLs target ~20% of all proteins for proteasomal degradation (5). In general, CRLs consist of four proteins: Rbx (RING box) protein, cullin proteins, adaptor proteins, and substrate-binding proteins (SBPs). Fig. 1 presents a schematic diagram of CRL. Previously, we proposed that CRL works as a two-arm machine, which includes the SBP and Rbx arms (6–8). Flexible linkers exist in both arms, and these help to bring E2 and the substrate into proximity to facilitate ubiquitination. The cullin proteins serve as a scaffold that connects these two arms.

The members of the cullin family are evolutionarily conserved (4). There are three cullins in yeast, six in *Caenorhabditis elegans*, five in *Drosophila*, five in *Arabidopsis*, and eight in mammals (9). The human genome encodes six canonical human cullin proteins (Cul1, Cul2, Cul3, Cul4A, Cul4B, and Cul5) and three atypical cullin proteins (Cul7, PARC, and APC2), which are partially conserved with the canonical human cullins (4, 9–11).

* This work was supported, in whole or in part, by National Institutes of Health Contract HHSN261200800001E from NCI and the National Cancer Institute Center for Cancer Research Intramural Research Program of the National Institutes of Health.
⌘ *Author's Choice*—Final version full access.
[S] The on-line version of this article (available at http://www.jbc.org) contains supplemental Fig. S1.
[1] To whom correspondence should be addressed. Tel.: 301-846-5579; E-mail: ruthnu@helix.nih.gov.

[2] The abbreviations used are: CRL, cullin-RING E3 ubiquitin ligase; SBP, substrate-binding protein; NTD, N-terminal domain; CTD, C-terminal domain.

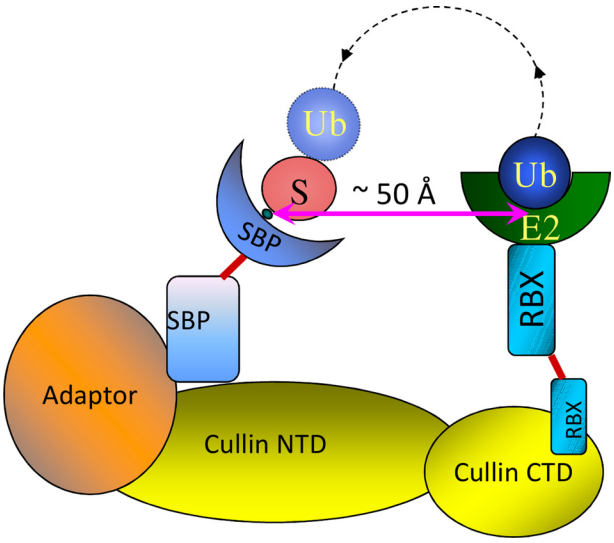

FIGURE 1. **Schematic drawing of the CRL machine.** On the left arm, *S* stands for substrate. The distance gap between the binding site of the substrate-binding protein and E2 ubiquitin (*Ub*) is marked.

On the basis of sequence homology, the structures of the six canonical cullins are expected to be conserved. They include two domains: the N-terminal (NTD) and C-terminal (CTD) domains (11). The NTD is stalk-like and consists of three repeats. The CTD is globular with a cullin homology domain signature. Via repeat 1, the NTD recognizes different adaptor proteins and SBPs, which bind to different substrates, whereas the CTD binds to Rbx proteins, which bind to E2 and ubiquitin. Via the adaptor protein Skp1 (12) Cul1 specifically connects to F-box proteins, including Skp2 (13), Fbw7 (14), β-TrCP1 (15), Cdc4 (16), etc. Cul2 and Cul5 bind to the same adaptor proteins, elongins B and C (17, 18). Via elongin B/C, Cul5 connects to SOCS-box proteins, such as SOCS2 (19), SOCS4 (20), Vif (21, 22), etc., and Cul2 connects to VHL-box proteins, such as pVHL (23, 24). The adaptor protein for Cul4A/Cul4B is DDB1 (damaged DNA-binding protein 1) (25). DCAF (DDB1- and Cul4A-associated factor) (26) or DWD (DDB1-binding WD40) (25) proteins are identified as SBPs for Cul4A. Distinct from other cullins, the adaptor and SBP for Cul3 is one single protein, identified as BTB domain protein (27).

The SCF^{Skp2} model reveals a 50-Å gap between the substrate-binding site and the E2 active site (Fig. 1) (12). How does CRL bridge this distance gap? We previously proposed that CRL works as a two-arm machine and that both arms are flexible, allowing this distance to be bridged (6–8). However, what is the role of the cullins? Do the cullins serve only as a rigid scaffold for ubiquitination? It is known that six human cullins target specific adaptors and SBPs. The sizes of the adaptors and SBPs are different, but the structures of the cullins are conserved. If the cullins are rigid, how do they specifically accommodate adaptors and SBPs with different sizes? Here, via structural analysis and molecular dynamics simulations, we demonstrate that Cul1, Cul4A, and Cul5 are not rigid. Instead, these three cullins are flexible scaffolds with preferred distributions of conformational states that allow the CRLs to increase the E2-substrate distance to a specific range and, in this way, facilitate polyubiquitination.

EXPERIMENTAL PROCEDURES

System Setup—The starting structures of the unbound Cul1 form and Cul1-Rbx1 complex were extracted from the Rbx1-Cul1-Skp1-$Skp2^{F\text{-}box}$ complex structure (Protein Data Bank code 1ldk (12)). The Cul1 structure from Cand1-Cul1-Rbx1 (Protein Data Bank code 1u6g (28)) was used for structure comparison. The initial structures of the unbound Cul4A form and Cul4A-Rbx1 complex were extracted from the DDB1-Cul4A-Rbx1-SV5V complex (Protein Data Bank code 2hye (25)). The CTD of Cul5 was taken from the closed form of $Cul5^{CTD}$-Rbx1 (Protein Data Bank code 3dpl (29)). The homology model of the human NTD of Cul5 was built with SWISS-MODEL (30) based on the crystal structure of the mouse Cul5 NTD (Protein Data Bank code 2wzk) because the sequence identity of the human and mouse Cul5 NTDs is as high as 95%. The interface between the NTD and CTD of Cul5 was constructed based on the Cul1 crystal structure. The starting structures for the mutants were constructed by substituting the long loop of Cul1/Cul5 with the corresponding short loop of Cul4A. The missing residues in the starting structures were added as random coils and minimized for 5000 steps with the steepest descent method, followed by another 5000-step minimization with the adopted basis Newton-Raphson method. A TIP3P water box was constructed with a minimum distance of 12 Å from the edge of the box to any protein atom. The system was neutralized, and the ionic concentration was kept at 0.5 mol/liter by adding sodium and chloride ions. The sequence and structure analyses were performed using BLAST (31) and VMD (32), respectively.

Simulation Protocol—Molecular dynamics simulations were performed with explicit solvent using the NAMD2.7 program (33). The Charmm27 force field (34) was used. First, we minimized the solvated systems for 5000 steps with the protein restrained, followed by another 5000 steps with all atoms set free. The systems were heated to 300 K in 500 ps and equilibrated for 500 ps with the protein backbone atoms constrained to allow relaxation of the solvent, followed by a 1-ns equilibration run without any constrains. We then performed production runs for 60 ns with the NPT ensemble. Two independent trajectories were performed for each wild-type state. During the production run, the pressure was maintained at 1 bar using the Nosé-Hoover Langevin piston barostat, and the temperature was controlled at 300 K with a Langevin thermostat. We used particle mesh Ewald summation to treat long-range electrostatic interactions. For the short-range non-bonded interactions, we employed a switch function with a cutoff of 12 Å and a switching distance of 10 Å. The time step was set as 2 fs with a SHAKE constraint on all bonds containing hydrogen atoms. We restrained the distance between the Rbx1 RING finger zinc atoms and their neighboring atoms during the equilibration and production runs. VMD (32) and Hingefind (35) were used for the rotation angle analyses.

Model Setup—We built the model for CRL1 ubiquitination by docking E2 UbcH7 (Protein Data Bank code 1fbv (36)) and superimposing the F-box of β-TrCP1 (Protein Data Bank code 1p22 (15)) with the Rbx1 RING subdomain and the F-box of Skp2, respectively, of the Rbx1-Cul1-Skp1-$Skp2^{F\text{-}box}$ complex (Protein Data Bank code 1ldk (12)). For the CRL5 ubiquitina-

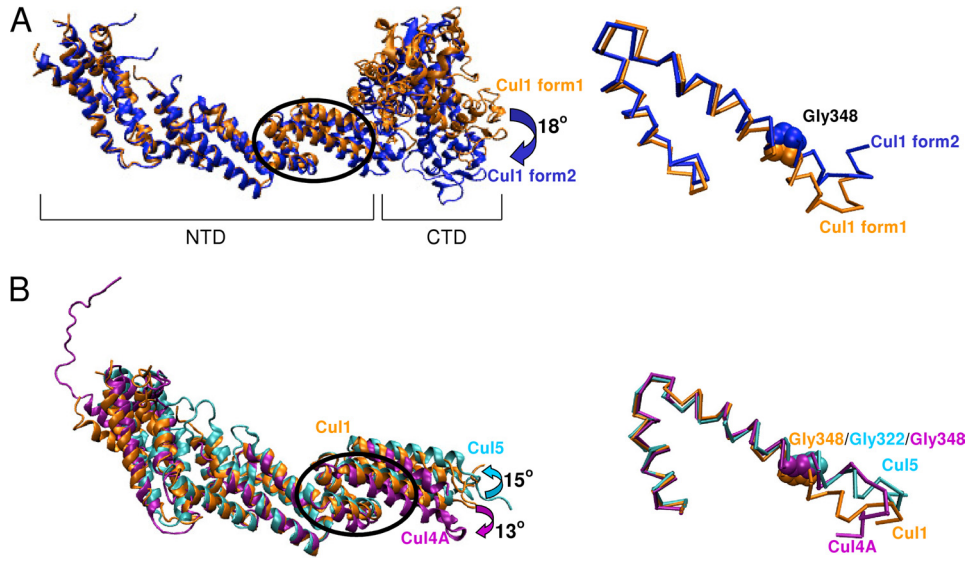

FIGURE 2. **Structural analysis of Cul1, Cul4A, and Cul5.** *A*, alignment of two Cul1 forms from different complexes. Form 1 (*orange*) is taken from Rbx1-Cul1-Skp1-Skp2 (Protein Data Bank code 1ldk), and Form 2 (*blue*) is from Cand1-Cul1-Rbx1 (code 1u6g). The region containing the rotation hinge is *circled*, and the details are shown on the right. The Gly-348 hinge is labeled. *B*, alignment of Cul1, Cul4A, and Cul5 NTD. Cul1 (*orange*) is taken from Rbx1-Cul1-Skp1-Skp2 (Protein Data Bank code 1ldk) complex, Cul4A (*purple*) is extracted from Cul4A-Rbx1-DDB1-SV5V (code 2hye), and the Cul5 NTD was crystallized separately (code 2wzk). The region with the rotation hinge is *circled*, and the details are shown on the right. The Gly-348 (Cul1), Gly-322 (Cul5), and Gly-348 (Cul4A) hinges are labeled.

tion model, we docked E2 UbcH7 into the Cul5-Rbx1 complex (Protein Data Bank code 3dpl (37)) and superimposed the elongin B/C and SOCS2 SOCS-box domain with the Skp1 and Skp2 F-box domains, respectively. For the CRL4A model, E2 UbcH7 was docked into Rbx1 in the DDB1-Cul4A-Rbx1-SV5V complex (Protein Data Bank code 2hye (25)).

RESULTS

Flexible Hinges Exist in the NTDs of Cul1, Cul4A, and Cul5—Two x-ray crystal forms for Cul1 are available in the Protein Data Bank. These two Cul1 crystal forms have conserved structures, including the NTD and CTD. One Cul1 conformation form (Form 1, Protein Data Bank code 1ldk) is bound to Skp1/Skp2 at the NTD and to Rbx1 at the CTD, and the other Cul1 conformation form (Form 2, Protein Data Bank code 1u6g) is bound to Cand1 at both domains and to Rbx1 at the CTD. These two forms have similar overall structures with a root mean square deviation of 3.2 Å for the Cα atoms. In both crystal forms, the NTD consists of three repeats with similar structures. Whereas repeats 1 and 2 are well aligned with each other, when the two Cul1 structures are superimposed, repeat 3 in Form 2 is tilted by 15° compared with Form 1. The alignment is shown in Fig. 2. Compared with Form 1, the angle of Asn-347–Gly-348–Leu-349 Cα changes by 18°, from 80° (Form 1) to 98° (Form 2), suggesting that Cul1 may not be rigid but flexible with Gly-348 serving as the hinge. It is known from the crystal structure of Cul1 that the distance gap between E2 and the substrate is ~50–60 Å, but this 18° tilt angle can increase this distance gap significantly. When Cul1 Form 1 was substituted with Form 2, the distance gap between β-TrCP1 and E2 increased significantly from 54 Å (Form 1) to 66 Å (Form 2), suggesting that cullin flexibility may play an important role in ubiquitination.

The structures of the NTD and CTD of Cul5 were solved separately. The Protein Data Bank code for the NTD is 2wzk. The NTDs of Cul5 and Cul1 are conserved in sequence and structure. They have 25% sequence identity and 48% sequence similarity. Both structures have the same architecture with three repeats. The overall root mean square deviation is 3.1 Å. However, when the Cul5 and Cul1 NTDs are superimposed, a tilt angle of 15° is observed. The hinge is at Cul5 Gly-322 or Cul1 Gly-348 at repeat 3, implying that Cul5 might also be flexible.

The complex structure of DDB1-Cul4A-Rbx1 hijacked by the V protein of simian virus 5 was solved. The overall structure of Cul4A is conserved compared with those of Cul5 and Cul1. The NTD root mean square deviations are 3.1 and 2.4 Å compared with Cul5 and Cul1, respectively. However, the tilt angles with the hinges located in repeat 3 at Gly-348 are observed when Cul4A is aligned with either Cul1 or Cul5. More interestingly, sequence analyses showed that the Gly hinge is conserved in cullins.

On the basis of the above structural analysis of crystal structures, we hypothesized that Cul1, Cul4A, and Cul5 are not rigid and that flexible hinges may exist in the NTDs of these cullins. To test our hypothesis, we performed molecular dynamics simulations for the unbound forms of Cul1, Cul4A, and Cul5. Two separate trajectories were performed for each cullin, with each trajectory running for 60 ns. As we expected, all of the simulations indicate a flexible rotation angle, as shown in Fig. 3. However, the hinges for Cul1, Cul5, and Cul4A are distinct. The hinge is at Gly-212 on repeat 2 for Cul1, at Gly-328 on repeat 3 for Cul5, and at Gly-306 on repeat 3 for Cul4A (Fig. 3). The dihedral angles at the hinges during the simulations are shown in supplemental Fig. S1. The blast hits of 44 sequences of cullins, including Cul1, Cul2, Cul3, Cul4A, Cul4B, and Cul5 in different species, show that Gly-212 on repeat 2 is 52% conserved. Gly-306 and Gly-328 in repeat 3 are 100% conserved in all 44 sequence hits.

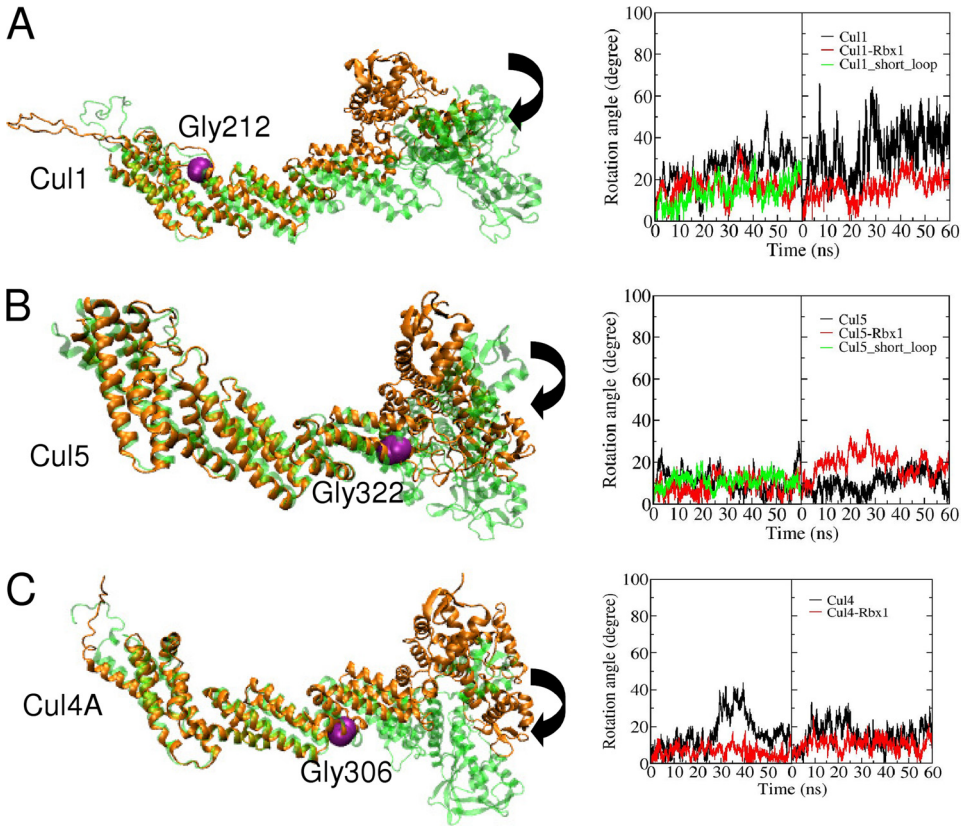

FIGURE 3. **Conformational changes in Cul1, Cul4A, and Cul5 during the simulation.** Images at 0 ns (*orange*) and the image with the maximum rotation angles are superimposed for the unbound states of Cul1 (*A*), Cul5 (*B*), and Cul4A (*C*), as shown on the left. The hinges detected during the simulations are shown in *purple* and are labeled. Rotation angles from two separate trajectories are shown on the right. The unbound states are shown as *black lines*, the Rbx1-bound states as *red lines*, and mutants with a shorter loop as *green lines*.

The rotation angles are also distinct for these three cullins. Cul1 has the largest rotation angles, with a maximum at 66° and an average of 29° (Fig. 3*A*). The maximum rotation angle for Cul5 is the smallest, at 30°, and the average rotation angle is 10.5° (Fig. 3*B*). The rotation angle of Cul4A is between those of Cul1 and Cul5, with a maximum at 44° and an average of 16° (Fig. 3*C*). These simulation results suggest that cullin NTD flexibility is a common and intrinsic feature for Cul1, Cul5, and Cul4A, but the degrees of flexibility are distinct among these three cullins.

Distance Gaps Are Distinct for Cul1, Cul4A, and Cul5—Cul1, Cul4A, and Cul5 recognize specific adaptor proteins and different SBPs. These proteins have different shapes and sizes. We measured the distance between the substrate-binding and E2 ubiquitin-binding sites during the simulations for the unbound forms. We noticed that the distance gaps are distinct for Cul1, Cul4A, and Cul5, as shown in Fig. 4. For Cul1, the adaptor protein is Skp1, and the SBPs are F-box proteins. β-TrCP1 is used as an example here. The distances fluctuate from 21 to 75 Å. For Cul5, the adaptor proteins are elongins C and B, and the SBPs are SOCS-box proteins. SOCS2 is used as an example here. The distances fluctuate between 55 and 101 Å. For Cul4A, the adaptor protein is DDB1, and the substrate proteins are DWD proteins. SV5V is used as an example here. The distance fluctuates between 39 and 115 Å. The differences in the distance range between these three proteins suggest that different cullins present different degrees of flexibilities, which allow them to adjust the distance gap and accommodate different sizes of substrates.

Cullin NTD Flexibilities Still Exist When Bound to Rbx1—All three cullins bind to Rbx1 via their CTDs. Molecular dynamics simulations were performed for Cul1, Cul4A, and Cul5 when bound to Rbx1. In all three cases, flexibilities were still observed, even though binding of Rbx1 to the CTDs of Cul1 and Cul4A allosterically decreased the NTD rotation angles, as shown in Fig. 3. For Cul1, the largest rotation angle decreases by 29°, from 66° (unbound form) to 37° (Rbx1-bound form). For Cul4A, the largest rotation angle decreases by 26°, from 44° (unbound form) to 18° (Rbx1-bound form). These reduced rotations suggest that Rbx1 may allosterically decrease the flexibility of the Cul1 and Cul4A NTDs. There is no significant change and even a slight increase in the rotation angles for Cul5, with the largest rotation angles for the unbound and bound states being 30° and 36°, respectively, suggesting that Rbx1 binding to the Cul5 CTD has a minimum effect on the NTD.

The correlated motions are distinct for different cullins as well as for the unbound and bound states, as shown in Fig. 5. For Cul1, compared with the unbound state, in the bound form, NTD repeat 1 is more negatively correlated with the CTD but more positively correlated with NTD repeats 2 and 3. For Cul5, no significant changes were observed between the correlations within the NTD, but binding to Rbx1 significantly reduced the negative correlation between the NTD and CTD. The effects of Rbx1 binding to Cul4A differ from those to Cul1 and Cul5:

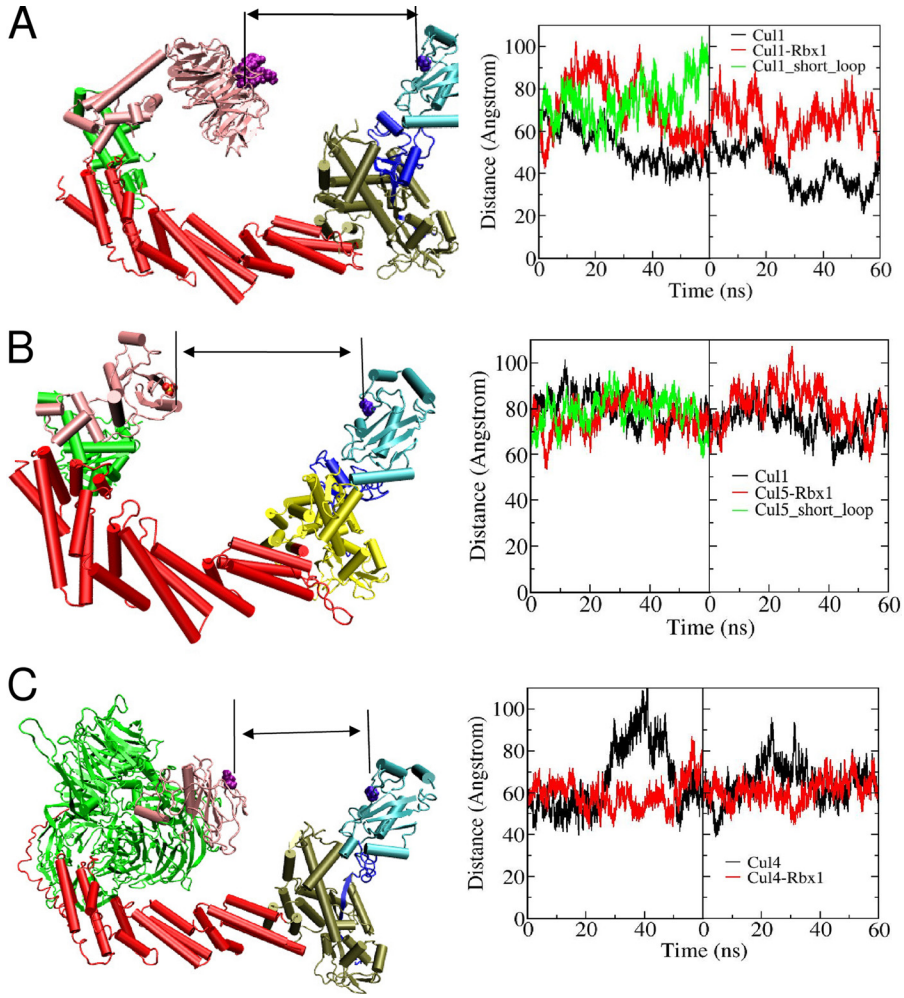

FIGURE 4. **Distances between E2 and SBPs fluctuate during simulations.** *A*, model of β-TrCP1-Skp1-Cul1-Rbx1-E2. β-TrCP1 is shown in *pink*, Skp1 in *green*, the Cul1 NTD in *red*, the CTD in *gold*, Rbx1 in *blue*, and E2 in *cyan*. *B*, model of SOCS2-elongin B/C-Cul5-Rbx1-E2. SOCS2 is shown in *pink*, elongin B/C in *green*, the Cul5 NTD in *red*, the CTD in *gold*, Rbx1 in *blue*, and E2 in *cyan*. *C*, model of SV5V-DDB1-Cul4A-Rbx1-E2. SV5V is shown in *pink*, DDB1 in *green*, the Cul1 NTD in *red*, CTD in *gold*, Rbx1 in *blue*, and E2 in *cyan*. The measured distances are illustrated. The distances during the simulation are shown on the right. The distances observed in the unbound states are shown as *black lines*, the Rbx1-bound states as *red lines*, and mutants as *green lines*.

there is more positive correlation within the NTD and less negative correlation between the NTD and CTD. In general, Rbx1 binding to Cul1 and Cul4A, but not to Cul5, changes the correlation within the NTD, making it more positive. This suggests that Rbx1 allosterically changes the NTD flexibility of Cul1 and Cul4A but has less effect on Cul5. This is consistent with our rotation analysis, which showed that Rbx1 binding has a lesser allosteric effect on Cul5 NTD rotation compared with Cul1 and Cul4A. On the other hand, binding to Rbx1 makes the correlated motions between the NTD and CTD more negative for Cul1 but less negative for Cul5 and Cul4A, again suggesting different allosteric effects for these three cullins.

We measured the distances between the SBP substrate-binding and E2 ubiquitin-binding sites during the simulations of these three cullins when bound to Rbx1. Compared with the unbound form, the distances are significantly increased for the bound Cul1 form. The distance range changed from 21–75 to 40–102 Å. For Cul4A, the distance range decreased, from 39–115 to 42–87 Å, but for Cul5, no significant changes were observed. The distance ranges for the unbound and bound forms are 55–101 and 53–107 Å, respectively. These results suggest that binding to Rbx1 allosterically adjusts the E2-substrate distance for Cul1 and Cul4A, accommodating substrates with different shapes and sizes, but Rbx1 binding to Cul5 has minimum allosteric effects in adjusting the E2-substrate distances.

Cullins Have Specific Distance Gaps for Specific Adaptors/SBPs—It is known that Cul1, Cul4A, and Cul5 all have specific adaptors and SBPs. The specific adaptors for Cul1, Cul4A, and Cul5 are Skp1, DDB1, and elongin B/C, respectively, whereas the SBPs are F-box, DWD, and SOCS-box proteins, respectively. To determine whether these adaptors and SBPs can substitute for one another, we measured the E2-distance gap for all three cullins with each of the adaptors/SBPs during the simulations of the Rbx1-bound state. The results are shown in Fig. 6. For β-TrCP1 and Skp1, the distance gap distribution is in a different range for Cul1, Cul4A, and Cul5. The peak in the distance distribution is at ~70 Å for Cul1 but is 20 Å shorter or longer for Cul5 and Cul4A, respectively. This suggests that each cullin presents specific flexibility (*i.e.* preferred distribution of conformational states), which allows it to maintain a specific distance range. For Cul1, this may be important

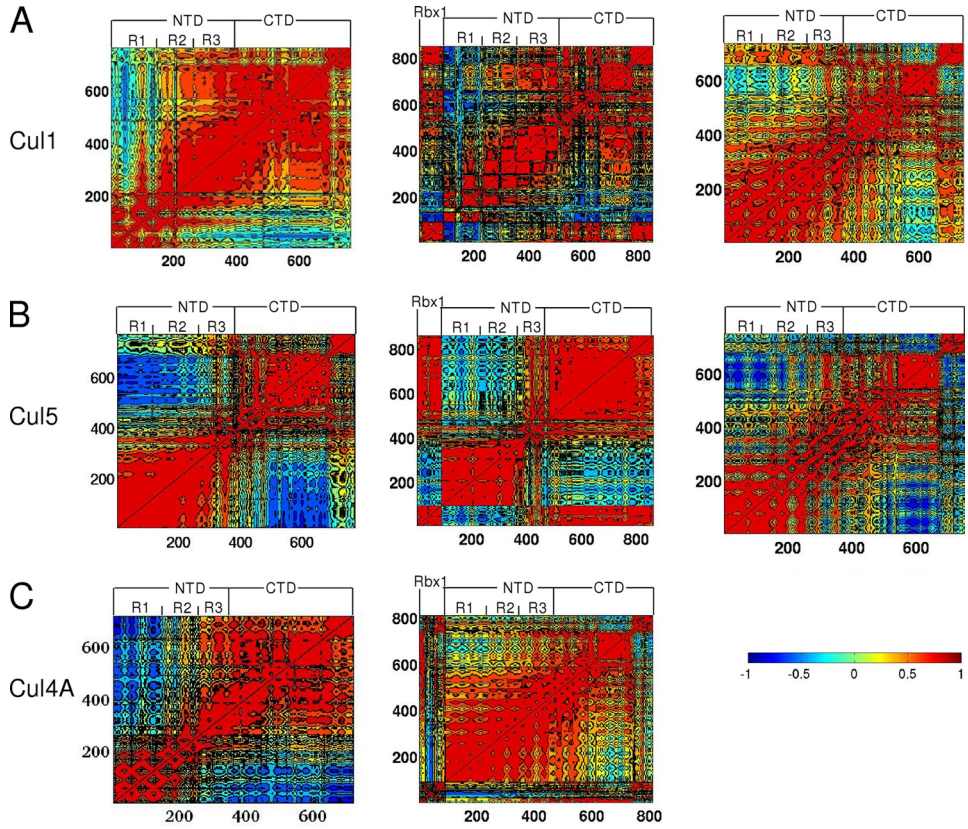

FIGURE 5. **Distinct covariance maps of Cul1, Cul4A, and Cul5.** *A*, Cul1; *B*, Cul5; *C*, Cul4A. The unbound states are shown in the *left panels*, the Rbx1-bound states in the *middle panels*, and the mutants in the *right panels*. The more *red*, the stronger the positive correlation; the more *blue*, the stronger the negative (anti) correlation. The *bar* provides the scale.

for its function with Skp1/β-TrCP1. Similar to Cul1, the peak in the Cul5 distance distribution is at ~70 Å for its specific adaptor elongin B/C and its SBP SOCS2; however, the distributions are quite different for Cul1 and Cul4A. On the other hand, the distance peaks for these three cullins with DDB1/SV5V are quite close. It seems that from the flexibility standpoint, Cul1 and Cul5 could substitute for Cul4A in targeting DDB1/SV5V; however, from the structural standpoint, considering that Cul4A has a specific NTD structure that allows it to bind to DDB1, Cul1/Cul5 cannot bind to DDB1. Overall, this distance analysis suggests that Cul1, Cul4A, and Cul5 bind to specific adaptors and SBPs, allowing them to maintain the E2-substrate distance in a specific range to facilitate ubiquitination.

Deletion of the Cul1 Loop Allosterically Changes the Behavior of the NTD—Comparing the sequences and structures of Cul1, Cul5, and Cul4A, we noticed that even though these three cullins are highly similar, Cul1 and Cul5 have unique loops. Cul1 has a long loop in repeat 1, whereas Cul5 has a long loop between the NTD and CTD. We suspected that the different behavior of the cullins could be attributed to these loops. To test this assumption, we deleted the long loops of Cul1 and Cul5 and substituted them with the corresponding short loop from Cul4A. Molecular dynamics simulations were then performed to test the effects of these mutations.

In the unbound forms, the behavior of the Cul1 mutant with shorter loop changed significantly compared with the WT. More interestingly, the behavior of the unbound mutant form was more similar to that of the Rbx1-bound WT form. The largest rotation angle of the Cul1 mutant decreases (Fig. 3) to 32°, a significant decrease compared with 66° in the unbound WT form but similar to the maximum rotation angle of the bound WT form, which is 29°. The correlation map changes accordingly. The correlation between repeats 1 and 2 becomes more positive compared with the unbound WT form. The distance gap range is 50–105 Å, which is a significant increase compared with 21–75 Å of the unbound WT form but similar to 40–102 Å of the bound WT form.

Unlike the Cul1 mutant, the Cul5 mutant with a shorter loop does not show a significant change compared with either the unbound or bound WT form. For the Cul5 mutant, the maximum rotation angles is 21°, and the distance gap range is 58–97 Å, both of which are similar to those of the unbound and bound WT forms. Thus, the alteration of the loop length leads to conformational and dynamic changes far away, suggesting that the loop plays an allosteric role.

DISCUSSION

Cullins have long been believed to serve as a rigid scaffold in CRLs. A major reason for this is that the crystal structures of Cul1, Cul4A, and Cul5 are conserved, implying cullin rigidity. Another piece of evidence supporting the rigidity of cullins has been provided by Zheng *et al.* (12). These authors added an artificial linker at the interface between the NTD and CTD and discovered that the mutant with the artificial linker failed to ubiquitinate the substrate *in vitro*, suggesting that the rigidity of Cul1 is important for ubiquitination. However, the small angle

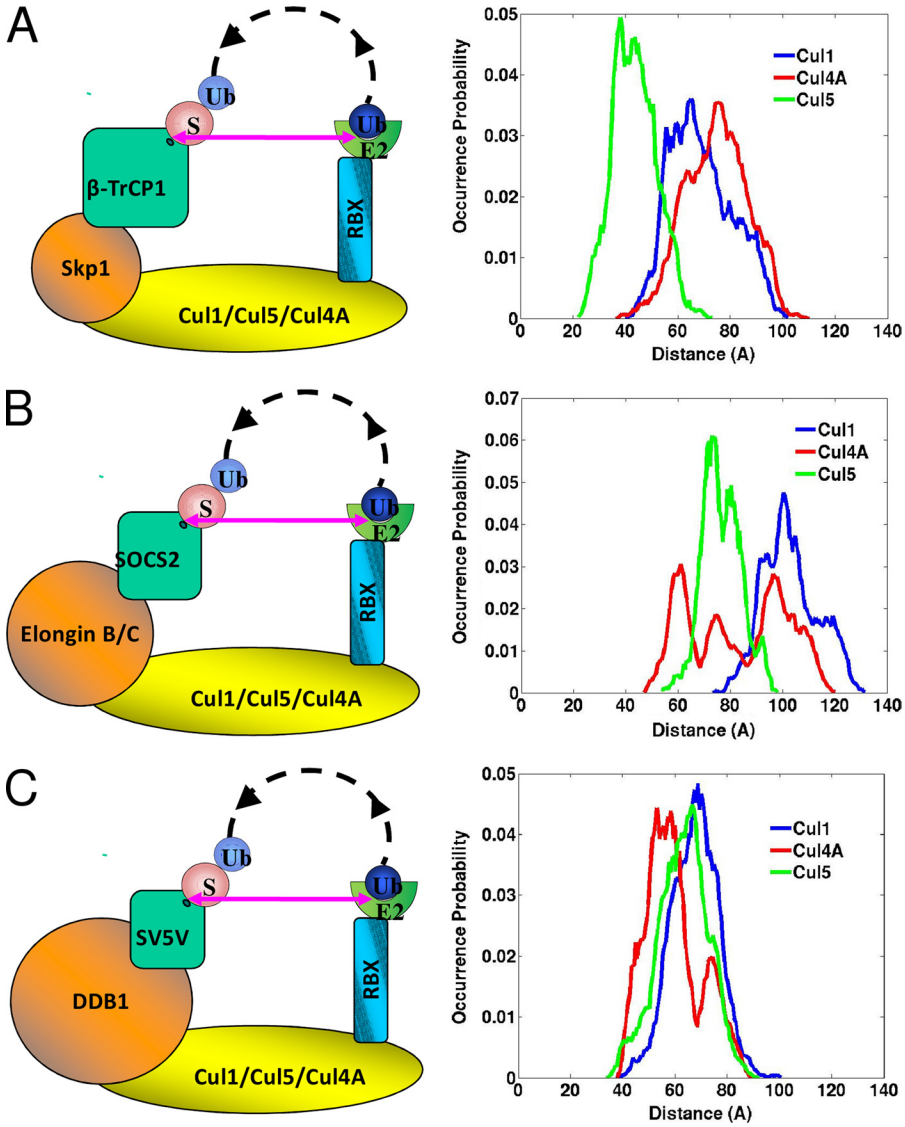

FIGURE 6. **Distance ranges are distinct for specific adaptors/SBPs.** The distance ranges for Cul1, Cul4A, and Cul5 when bound to Rbx1 and Skp1/β-TrCP1 (*A*), elongin B/C/SOCS2 (*B*), and DDB1/SV5V (*C*) are shown. *S*, substrate; *Ub*, ubiquitin.

x-ray scattering data on $Cul1^{CTD}$-Rbx1 showed that $Cul1^{CTD}$-Rbx1 is flexible (37), and we previously reported that $Cul5^{CTD}$ is flexible (8). In this study, we demonstrated that the cullin NTDs are not rigid scaffolds but are also flexible enough to facilitate ubiquitination.

We previously observed flexible linkers in both SBPs and Rbx proteins. Even though cullins include two domains, no flexible linkers are observed between the NTD and CTD, which is consistent with experiments showing that an artificial NTD-CTD linker disrupts cullin function (12). However, our analysis of the two crystal structures of Cul1 in two complexes, Cul1-Rbx1-Skp1-Skp2 and Cand1-Cul1-Rbx1, showed a tilt angle of 18° and a hinge at Gly-348 in the NTD. Cand1 is a cellular inhibitor that inhibits ubiquitination. This tilt angle may suggest that Cul1 can be flexible and adopt a different conformation when activated and inhibited by Cand1. When we performed molecular dynamics simulations, we noticed different hinges: Gly-212 in repeat 2 for Cul1 and Gly-306 and Gly-322 in repeat 3 for Cul4A and Cul5, respectively. More interestingly, these glycines are conserved, especially Gly-306 and Gly-322, which are 100% conserved in all cullin types and in all species, suggesting that cullin flexibility could be an intrinsic and common feature for all cullins.

In our previous work (6), we superimposed the box domain of F-box proteins and found that the substrate-binding sites overlap in space. A similar overlap was observed for SOCS-box and VHL-box proteins. However, when we superimposed the box domain of F-box proteins with SOCS/VHL-box proteins, the substrate-binding sites are far away from each other. F-box and SOCS/VHL-box proteins have different sizes. F-box proteins have >400 residues, but SOCS/VHL-box proteins have <250 residues. F-box, SOCS-box, and VHL-box proteins bind to different cullins, and the cullins may recognize specific SBPs via sequence and structural diversity of NTD repeat 1, which contains the binding sites for the adaptors, and these contain the binding sites for SBPs. For example, it was reported that specific sequences in Cul2 VHL- and Cul5 SOCS-binding sites determine the specific recognition (17, 18). Another example is

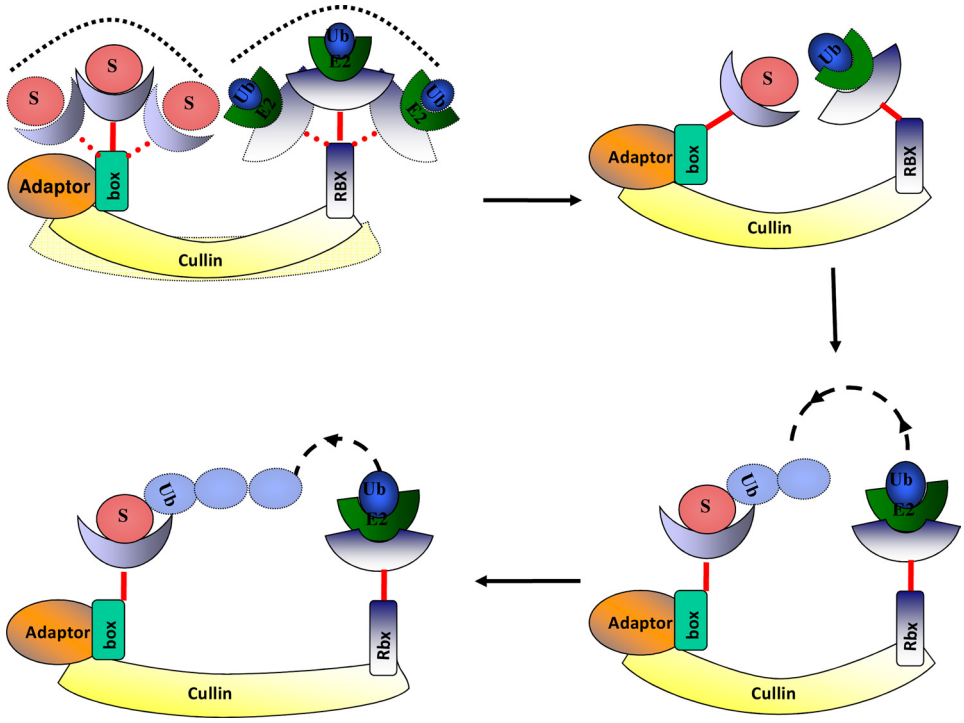

FIGURE 7. **Proposed scheme of the flexible two-arm machine for the CRL mechanism.** *Upper left*, a large ensemble of conformations exists, with flexible Rbx, SBPs, and cullins. *Upper right*, shifts of the populations of the ensemble to the favorable conformation for initiation of ubiquitination. *Lower right*, shifts of the ensemble population again for chain elongation. *Lower left*, population shift in the cullin for formation of longer ubiquitin chain. *S*, substrate; *Ub*, ubiquitin.

Cul4A, which has a specific N-terminal extension sequence that recognizes DDB1 as its adaptor (25). However, one question remains unclear: how do the cullins, with conserved structure, accommodate SBPs with distinct shapes and sizes? Here, we propose that the flexibility of the cullin NTDs, either in their unbound form or when bound to Rbx1, differ and that this difference helps in maintaining the optimum E2-substrate distance gap for the ubiquitination of the different adaptors/SBPs.

In our previous "two-arm machine" model, we proposed that SBPs and Rbx1 serve as two arms in the CRL machine. Both arms are flexible, which allows initiation and ubiquitin chain elongation. The flexibilities of these two arms increase the probability of substrate ubiquitination. However, the sizes and shapes of the SBPs and substrates are all distinct. To ubiquitinate substrates with different sizes and shapes efficiently, CRL needs both flexibility and conformational control of the flexibility (38). As shown by Zheng *et al.* (12), the artificial flexible linker between the Cul1 CTD and NTD disrupts ubiquitination. This observation can be explained: an artificial linker would increase CRL flexibility. This is important because if the cullin is rigid, the likelihood of reaching the optimum position for ubiquitination may not be sufficiently high. However, at the same time, a conformational ensemble that is too large would decrease the ubiquitination efficiency (38). Here, we have demonstrated that the flexible cullins allosterically control the distances between E2 and their specific target in the optimum range, which increases the efficiency of ubiquitination, *i.e.* they bias the distribution of the ensemble toward the ubiquitination-favored states. The physiological significance of our finding lies in the mechanism it provides, which illustrates how CRLs can accurately perform their function for substrates with different sizes and shapes.

On the basis of our results and experimental data, we now go beyond our previously proposed model and propose a new "flexible two-arm machine" model that can explain how the CRL facilitates ubiquitination (Fig. 7). We suggest that the cullins serve as a flexible, allosterically controlled scaffold for the CRL machine. Both the NTD and CTD of cullins are flexible. The NTD flexibility suggests that there exists an ensemble of cullin conformations. The CTD flexibility, together with the Rbx1 flexibility, which is regulated by the allosteric effect elicited by neddylation, helps to juxtapose the E2-substrate active sites. Cullins serve as a flexible, conformationally controlled scaffold that ensures that sufficient space is available for an efficient mono- and polyubiquitination CRL machine. The flexibilities of the two arms that contain the SBPs and Rbx proteins facilitate the transfer of the first ubiquitin from E2 to the substrate in monoubiquitination. In polyubiquitination, the population shift in the cullin conformational ensemble and in the two arms accommodates a long ubiquitin chain. The distribution of the ensemble allows the cullins to maintain the distance at a certain range: neither too large to ensure ubiquitination efficiency nor too small so as to hinder ubiquitin chain elongation. The flexibilities of the cullins are specific for different cullins to accommodate specific adaptors, SBPs, and substrates.

In our mechanism, there are still a few unanswered questions. One relates to how ubiquitination is activated. We propose that substrate binding can activate cullin, but how substrate binding allosterically activates cullin is still unclear. Another question relates to the role of the adaptors. One obvious role is to connect cullins and SBPs. Crystal structures show large conformational changes for DDB1, the Cul4 adaptor, before and after binding to SV5V (25, 39). Moreover, recently, hydrogen exchange mass spectrometry has shown that elongin

C is highly dynamic (40). The flexibilities of DDB1 and elongin C raise the question of whether the flexibility could be an intrinsic feature of adaptors, including Skp1. In addition, CRLs are modified by allosteric NEDD8 and Cand1 binding. The cullin CTD can form a covalent bond with NEDD8 ubiquitin-like protein via a lysine. This is called neddylation. Neddylation stimulates ubiquitination by increasing the flexibility of the Rbx protein and the cullin CTD and, in this way, confers specificity. Cand1 blocks the cullin-binding site to NEDD8, thus inhibiting neddylation. Our structural analysis showed that the two Cul1 structures, when in the CRL and when bound to Cand1, have an 18° tilt angle, suggesting that Cul1 is flexible. In particular, it is of interest to understand whether or how the flexibility of the cullin NTD could be allosterically regulated by neddylation or binding to Cand1. It is also unknown whether the Rbx1 conformation is broadly distributed in space or is biased toward ubiquitination-favored positions. On the basis of our findings that the flexible cullins maintain the E2-substrate distance in the optimum range, we hypothesize that the flexibility of the cullin NTD could be correlated with that of Rbx1, such that this E2-substrate distance is favorably maintained. We suggest that this will facilitate polyubiquitination following neddylation. Overall, we propose that cullins, together with SBPs and Rbx, allosterically regulate ubiquitination at every step (6–8), thus providing tight control of the CRL machine.

Acknowledgment—For this study, we used the high performance computational capabilities of the Biowulf Linux cluster at the National Institutes of Health (biowulf.nih.gov).

REFERENCES

1. Hershko, A., and Ciechanover, A. (1998) *Annu. Rev. Biochem.* **67,** 425–479
2. Liu, S., and Chen, Z. J. (2011) *Cell Res.* **21,** 6–21
3. Capili, A. D., and Lima, C. D. (2007) *Curr. Opin. Struct. Biol.* **17,** 726–735
4. Jackson, S., and Xiong, Y. (2009) *Trends Biochem. Sci.* **34,** 562–570
5. Soucy, T. A., Smith, P. G., Milhollen, M. A., Berger, A. J., Gavin, J. M., Adhikari, S., Brownell, J. E., Burke, K. E., Cardin, D. P., Critchley, S., Cullis, C. A., Doucette, A., Garnsey, J. J., Gaulin, J. L., Gershman, R. E., Lublinsky, A. R., McDonald, A., Mizutani, H., Narayanan, U., Olhava, E. J., Peluso, S., Rezaei, M., Sintchak, M. D., Talreja, T., Thomas, M. P., Traore, T., Vyskocil, S., Weatherhead, G. S., Yu, J., Zhang, J., Dick, L. R., Claiborne, C. F., Rolfe, M., Bolen, J. B., and Langston, S. P. (2009) *Nature* **458,** 732–736
6. Liu, J., and Nussinov, R. (2009) *PLoS Comput. Biol.* **5,** e1000527
7. Liu, J., and Nussinov, R. (2010) *J. Mol. Biol.* **396,** 1508–1523
8. Liu, J., and Nussinov, R. (2010) *Biophys. J.* **99,** 736–744
9. Sarikas, A., Hartmann, T., and Pan, Z. Q. (2011) *Genome Biol.* **12,** 220
10. Skaar, J. R., Florens, L., Tsutsumi, T., Arai, T., Tron, A., Swanson, S. K., Washburn, M. P., and DeCaprio, J. A. (2007) *Cancer Res.* **67,** 2006–2014
11. Zimmerman, E. S., Schulman, B. A., and Zheng, N. (2010) *Curr. Opin. Struct. Biol.* **20,** 714–721
12. Zheng, N., Schulman, B. A., Song, L., Miller, J. J., Jeffrey, P. D., Wang, P., Chu, C., Koepp, D. M., Elledge, S. J., Pagano, M., Conaway, R. C., Conaway, J. W., Harper, J. W., and Pavletich, N. P. (2002) *Nature* **416,** 703–709
13. Hao, B., Zheng, N., Schulman, B. A., Wu, G., Miller, J. J., Pagano, M., and Pavletich, N. P. (2005) *Mol. Cell* **20,** 9–19
14. Hao, B., Oehlmann, S., Sowa, M. E., Harper, J. W., and Pavletich, N. P. (2007) *Mol. Cell* **26,** 131–143
15. Wu, G., Xu, G., Schulman, B. A., Jeffrey, P. D., Harper, J. W., and Pavletich, N. P. (2003) *Mol. Cell* **11,** 1445–1456
16. Orlicky, S., Tang, X., Willems, A., Tyers, M., and Sicheri, F. (2003) *Cell* **112,** 243–256
17. Kamura, T., Maenaka, K., Kotoshiba, S., Matsumoto, M., Kohda, D., Conaway, R. C., Conaway, J. W., and Nakayama, K. I. (2004) *Genes Dev.* **18,** 3055–3065
18. Mahrour, N., Redwine, W. B., Florens, L., Swanson, S. K., Martin-Brown, S., Bradford, W. D., Staehling-Hampton, K., Washburn, M. P., Conaway, R. C., and Conaway, J. W. (2008) *J. Biol. Chem.* **283,** 8005–8013
19. Bullock, A. N., Debreczeni, J. E., Edwards, A. M., Sundström, M., and Knapp, S. (2006) *Proc. Natl. Acad. Sci. U.S.A.* **103,** 7637–7642
20. Bullock, A. N., Rodriguez, M. C., Debreczeni, J. E., Songyang, Z., and Knapp, S. (2007) *Structure* **15,** 1493–1504
21. Bergeron, J. R., Huthoff, H., Veselkov, D. A., Beavil, R. L., Simpson, P. J., Matthews, S. J., Malim, M. H., and Sanderson, M. R. (2010) *PLoS Pathogens* **6,** e1000925
22. Stanley, B. J., Ehrlich, E. S., Short, L., Yu, Y., Xiao, Z., Yu, X. F., and Xiong, Y. (2008) *J. Virol.* **82,** 8656–8663
23. Min, J. H., Yang, H., Ivan, M., Gertler, F., Kaelin, W. G., Jr., and Pavletich, N. P. (2002) *Science* **296,** 1886–1889
24. Liu, J., and Nussinov, R. (2008) *Proc. Natl. Acad. Sci. U.S.A.* **105,** 901–906
25. Angers, S., Li, T., Yi, X., MacCoss, M. J., Moon, R. T., and Zheng, N. (2006) *Nature* **443,** 590–593
26. Li, T., Robert, E. I., van Breugel, P. C., Strubin, M., and Zheng, N. (2010) *Nat. Struct. Mol. Biol.* **17,** 105–111
27. Xu, L., Wei, Y., Reboul, J., Vaglio, P., Shin, T. H., Vidal, M., Elledge, S. J., and Harper, J. W. (2003) *Nature* **425,** 316–321
28. Goldenberg, S. J., Cascio, T. C., Shumway, S. D., Garbutt, K. C., Liu, J., Xiong, Y., and Zheng, N. (2004) *Cell* **119,** 517–528
29. Duda, D. M., Borg, L. A., Scott, D. C., Hunt, H. W., Hammel, M., and Schulman, B. A. (2008) *Cell* **134,** 995–1006
30. Arnold, K., Bordoli, L., Kopp, J., and Schwede, T. (2006) *Bioinformatics* **22,** 195–201
31. Altschul, S. F., Gish, W., Miller, W., Myers, E. W., and Lipman, D. J. (1990) *J. Mol. Biol.* **215,** 403–410
32. Humphrey, W., Dalke, A., and Schulten, K. (1996) *J. Mol. Graph.* **14,** 33–38, 27–28
33. Phillips, J. C., Braun, R., Wang, W., Gumbart, J., Tajkhorshid, E., Villa, E., Chipot, C., Skeel, R. D., Kalé, L., and Schulten, K. (2005) *J. Comput. Chem.* **26,** 1781–1802
34. Brooks, B. R., Brooks, C. L., 3rd, Mackerell, A. D., Jr., Nilsson, L., Petrella, R. J., Roux, B., Won, Y., Archontis, G., Bartels, C., Boresch, S., Caflisch, A., Caves, L., Cui, Q., Dinner, A. R., Feig, M., Fischer, S., Gao, J., Hodoscek, M., Im, W., Kuczera, K., Lazaridis, T., Ma, J., Ovchinnikov, V., Paci, E., Pastor, R. W., Post, C. B., Pu, J. Z., Schaefer, M., Tidor, B., Venable, R. M., Woodcock, H. L., Wu, X., Yang, W., York, D. M., and Karplus, M. (2009) *J. Comput. Chem.* **30,** 1545–1614
35. Wriggers, W., and Schulten, K. (1997) *Proteins* **29,** 1–14
36. Zheng, N., Wang, P., Jeffrey, P. D., and Pavletich, N. P. (2000) *Cell* **102,** 533–539
37. Duda, D. M., Scott, D. C., Calabrese, M. F., Zimmerman, E. S., Zheng, N., and Schulman, B. A. (2011) *Curr. Opin. Struct. Biol.* **21,** 257–264
38. Ma, B., Tsai, C. J., Halilolu, T., and Nussinov, R. (2011) *Structure* **19,** 907–917
39. Li, T., Chen, X., Garbutt, K. C., Zhou, P., and Zheng, N. (2006) *Cell* **124,** 105–117
40. Marcsisin, S. R., and Engen, J. R. (2010) *J. Mol. Biol.* **402,** 892–904